Surface temperatures calculation method for high albedo road surfaces in permafrost regions

Simon Dumais and Guy Doré
Université Laval and Centre d'études nordiques, Québec, Québec, Canada

ABSTRACT
High albedo road surfaces can be used to reduce heat absorption in order to limit the degradation of the permafrost under paved embankments. A method is proposed to calculate the surface temperature pavements in permafrost regions. First, several practical methods to determine the albedo of the pavement are presented. Second, the required climatic data to use the model are discussed. A method to calculate the incoming solar radiation is presented. Then, an albedo based model using a simplified energy balance at the surface of the pavement is used to calculate the radiation index and surface temperature of the pavement. Finally, an index based on Stefan equation is proposed to assess the effectiveness of high albedo surfaces for the mitigation of permafrost degradation. Two working examples are also presented for Beaver Creek, Yukon and Iqaluit, Nunavut.

RÉSUMÉ
Les surfaces à albédo élevé permettent de réduire l'absorption de chaleur afin de limiter la dégradation du pergélisol sous-jacent aux remblais routiers revêtus. Une méthode est proposée afin de calculer la température superficielle de la chaussée en contexte nordique. Tout d'abord, les méthodes pouvant être utilisées afin de déterminer l'albédo de la chaussée sont présentées. Par la suite, la collecte des données climatiques nécessaires à l'utilisation du modèle ainsi que le calcul du rayonnement solaire incident sont discutés. Ensuite, un modèle se basant sur le bilan d'énergie à la surface de la chaussée est utilisé pour le calcul de l'indice de radiation et de la température superficielle de la chaussée. Finalement, un indice se basant sur l'équation de Stefan est proposé afin d'évaluer les bénéfices liés à l'utilisation des revêtements à albédo élevé comme technique de mitigation de la dégradation du pergélisol. Deux exemples d'utilisation de la méthode de calcul seront aussi présentés pour Beaver Creek, Yukon et Iqaluit, Nunavut.

1   INTRODUCTION

High albedo pavement surfaces have been studied for several decades as a mitigation technique for permafrost degradation under paved embankments. The albedo is a metric of solar reflectivity and is the ratio between the reflected and incident radiation. High albedo surfaces can efficiently reduce the surface temperature of the pavement by reflecting more of the incoming sunlight than traditional pavement materials thus reducing thaw penetration and thaw settlement of the embankment (Berg and Quinn 1977, Bjella 2013). The absence of simple and reliable calculation tools to assess the thermal benefits related to high albedo surfaces can partly explain their limited use in practice.

The objective of this paper is to propose a method for the calculation of surface temperature of pavements in permafrost regions. First, the model used by the method is introduced. Then, the calculation method is presented. The first step is the determination of the surface albedo. The second is the gathering of the climatic data needed by the model, i.e. air temperature, wind speed and incoming solar radiation. This step includes charts to compute the theoretical site specific incoming solar radiation. The following step is the calculation of the radiation index and of the surface temperature of the surface from a set of design charts supported by the previously mentioned model. An index based on Stefan equation is then proposed in order to assess the effectiveness of high albedo surfaces for the mitigation of permafrost degradation from the thawing and freezing season surface temperature of the pavement. Finally, two working examples of how to use the proposed method will be presented for Beaver Creek, Yukon and Iqaluit, Nunavut.

2   MODEL

The model used for the calculation of surface temperature of the pavement was proposed by Dumais (2014). It is based on a simplified energy balance at the surface of the pavement which includes shortwave and longwave radiation balance, forced and free convection, and heat exchanged by conduction between the pavement surface and the underlying embankment material. The model was validated using data from a test section built at the Beaver Creek test site along the Alaska Highway in the Yukon, Canada and is presented in the following equation:

$$0 = 0{,}89(1-a)q_{solar}$$
$$- \left[1{,}106\left(\frac{T_s+T_a}{2}\right)^{0,3} U^{0,5} + 0{,}745|T_s - T_a|^{0,3} \right](T_s - T_a)$$
$$- 5{,}68 \times 10^{-8}(0{,}85T_s^4 - 0{,}7T_a^4) \qquad [1]$$

where a is the albedo; q_{solar} is the incoming solar radiation (W/m^2); T_s and T_a are the surface and air temperature (K); and U is the wind speed (m/s).

The surface temperature can be calculated using equation 1 directly. Only four input parameters are required, i.e. the albedo of the surface and three climatic data: the incoming solar radiation, the air temperature and the wind speed.

Dumais (2014) observed that equation 1 yielded a very good precision when the absorbed solar radiation is over 30 W/m^2. However, for lower absorbed solar radiation Dumais (2014) proposes to use an n-factor to calculate the surface temperature from the air temperature. An n-factor of 0,9 was observed at Beaver Creek when solar radiation is below 30 W/m². The absorbed solar radiation is easily calculated from the albedo and the incoming solar radiation:

$$q_{abs} = (1 - a) \times q_{solar} \qquad [2]$$

The model was developed and validated using average values for the input climatic data. Time-step of any length can theoretically be used, but the model is more reliable for weekly or monthly values. It is not recommended to use hourly data because of the lack of a term accounting for the heat latency. Seasonal averages data such as the freezing and thawing index of the air can be used only when the daily average absorbed solar radiation doesn't fall below 30 W/m^2 within the studied period. When the solar radiation is lower than this threshold which often occurs during the freezing season in the artic, it is recommended to use the n-factor approach. In this article, the thawing season is defined as the period when air temperature is higher than 0°C.

3 CALCULATION METHOD OF SURFACE TEMPERATURE

3.1 Albedo of the pavement

Levinson et al. (2010a, 2010b) proposed a comprehensive two parts review on defining and measuring a metric that accurately predicts solar heat gain. For practical purposes, the albedo of the pavement can be defined as the clear sky air mass one global horizontal solar reflectance. Defined as such, the albedo can be used to accurately calculate the surface temperature of conventional and high albedo pavement surfaces. The albedo of the pavement can be measured either directly on an existing road surfaces or on laboratory samples. Albedo values can also be found in the literature for most conventional types of pavement.

3.1.1 Existing road surfaces

The albedo can be measured using the conventional pyranometer technique (ASTM-E1918). A pyranometer is a device equipped with a sensor that measures the solar radiation. To measure the albedo of a surface, the pyranometer is first pointed towards the sky to measure the incoming solar radiation, it is then pointed toward the surface to measure the reflected solar radiation. The ratio between reflected and incoming solar radiation is the albedo.

A few restrictions apply to the conventional pyranometer technique. Sunlight must be used as the source of radiation because of its particular spectral distribution. The sky must be clear as the presence of clouds affects the spectral distribution of the incoming solar radiation. The incident angle of the sun must be smaller than 45° which can be very restraining for the high latitude of regions where permafrost is found. Most of all, the targeted surface must be big enough to ensure that the solar radiation measured by the pyranometer is reflected mostly by the target. Indeed, a target with a 1.5 meter radius only yields a sensor-to-surface view factor of 90% for a typical pyranometer with a 1,5 cm radius sensor placed 50 cm above the target (Levinson et al. 2010b), i.e. 10% of the solar radiation measured by the pyranometer is reflected by the surroundings of the target. This can lead to an error if the albedo of the background is significantly different from the albedo of the target. A circular target with a diameter of more than 4 m or a square target of more than 4 m on a side is required to use the conventional pyranometer technique (ASTM-E1918). However, the sensor-to-surface view factor can be increased by placing the pyranometer closer to the target or by increasing the target size. Calculation of view factors, also referred as form factor, will be discussed in the next sub-section.

3.2 Laboratory samples

Alternative pyranometer techniques can be used to measure the albedo of laboratory samples and smaller experimental surfaces. The first alternative technique requires the use of masks with known albedo values (Akbari et al. 2008). In this technique, the surface with unknown albedo is alternatingly covered by matching size black and white masks. The solar radiation reflected for each configuration is measured. Then, the solar radiation reflected by the uncovered surface of unknown albedo is measured. The experimental setup must keep the same geometry in order to have a constant view factor for the three configurations. In theory, the surfaces can be infinitively small, but the imprecision grows as the size of the surface decreases. Surfaces with at least a 0.5 meter radius are thus recommended. For the alternative pyranometer technique, the albedo of the surface is calculated as such:

$$a = a_{black} + \frac{I_r - I_{r,black}}{I_{r,white} - I_{r,black}} (a_{white} - a_{black}) \qquad [3]$$

where a, a_{black} and a_{white} are the albedo of the surface with unknown albedo and of the black and white masks respectively; and I_r, $I_{r,black}$ and $I_{r,white}$ are the reflected solar radiation measured by the pyranometer for the target and for the black and white masks configurations respectively.

The second alternative pyranometer technique requires the calculation of form factors (Dumais 2014). Although it is less precise, this technique doesn't require the use of masks and yields sufficiently precise albedo values for the calculation of the surface temperature of pavements. First, the albedo of a uniform non-selective background such as tar paper is measured using the conventional pyranometer technique. The surface of

unknown albedo is then placed directly under the pyranometer sensor in the middle of the uniform background and the albedo of the composite surface is measured. The following equation is used to calculate the unknown albedo of the surface:

$$a = \frac{a_{composite} - a_{background}}{FF} + a_{background} \qquad [4]$$

where a, $a_{composite}$ and $a_{background}$ are the albedo of the surface with unknown albedo, of the composite surface and of the background respectively; and FF is the sensor-to-surface form factor of the surface with unknown albedo.

The sensor-to-surface form factor is a geometric factor that can be easily calculated using equations available in radiative heat transfer textbooks (Siegel and Howell 2002). An example of a disk-to-disk configuration for a typically round pyranometer sensor is presented in figure 1.
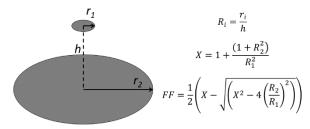

$$R_i = \frac{r_i}{h}$$

$$X = 1 + \frac{(1 + R_2^2)}{R_1^2}$$

$$FF = \frac{1}{2}\left(X - \sqrt{\left(X^2 - 4\left(\frac{R_2}{R_1}\right)^2\right)}\right)$$

Figure 1. Form factor for a disk-to-disk configuration

3.2.1 Literature values

Albedo values can be found in the literature for different types of pavements (Dumais 2014, Kilokotsa 2013). It is suggested to be cautious when using values from the literature as the albedo of a pavement depends not only on the reflective properties of the material but also on its age, texture and degradation state (Dumais, 2014).

3.3   Climatic data

In addition to the albedo of the pavement, three climatic data are required as input for the model: air temperature, wind speed and incoming solar radiation. The air temperature and the wind speed are usually readily available for a site where a thermal conception is required and thus won't be discussed in any details here. However, the incoming solar radiation is often unavailable. Fortunately, it can be calculated as it is mainly a function of the latitude of the site and of the time of year.

3.3.1 Calculation of incoming solar radiation

The incoming solar radiation reaching a surface at the surface of the earth is a function of extraterritorial solar radiation reaching the top of the atmosphere and of the radiation absorbed by the atmosphere.

Dumais (2014) proposed a series of convenient graphics to calculate the extraterritorial solar radiation (G_0) based on well-known geometric relationships found in the literature. Figure 2 presents the monthly extraterritorial solar radiation as a function of latitude. Figure 3 and 4 presents the thawing and freezing season

extraterritorial solar radiation as a function of latitude for different length of thawing and freezing season. Additional equations were also proposed by Dumais (2014) for the calculation of the extraterrestrial solar radiation of time-step of different length.
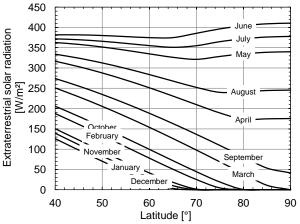

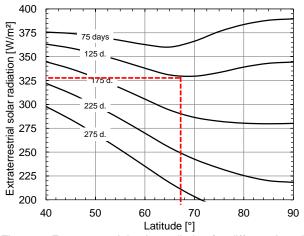Figure 2. Monthly extraterrestrial solar radiation

Figure 3. Extraterrestrial solar radiation for different length of thawing season (dashed line from example 5.2)
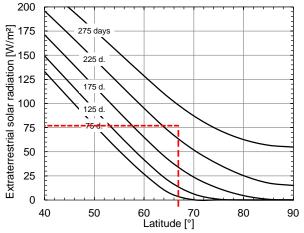

Figure 4. Extraterrestrial solar radiation for different length of freezing season (dashed line from example 5.2)

The incoming solar radiation at the surface of the earth can be calculated after part of the extraterritorial solar radiation has been scattered or absorbed by the atmosphere (Prescot, 1940):

$$q_{solar} = G_0(0{,}25 + 0{,}54 \times n/N) \qquad [5]$$

where q_{solar} is the incoming solar radiation at the surface of the earth; G_0 is the extraterritorial solar radiation; and n/N is the cloud factor.

The cloud factor is the ratio between the actual observed number of sunlight hours and the maximum theoretical number of sunlight hours. It is sometimes referred as the percentage of possible daylight hours. The cloud factor can be obtained for normal climatic data or it can be calculated from observations made on the field using measurements of incoming solar radiation compared with maximum theoretical values. The use of a high cloud factor is conservative and is thus recommended when the surface temperatures are used to calculate the maximum thaw depth under the pavement during the thawing season.

3.4 Surface temperature

It is possible to use equation 1 directly to calculate the surface temperature. A method based on graphic based calculation tools and the radiation index is also proposed here.

The radiation index (*RI*) is an alternative to the n-factor often used to convert the air temperature into surface temperature (Dysli, 1991). The *RI* was initially defined only for the freezing period as seen in equation 6. Its definition can be extended to the thawing period as well as shown in equation 7.
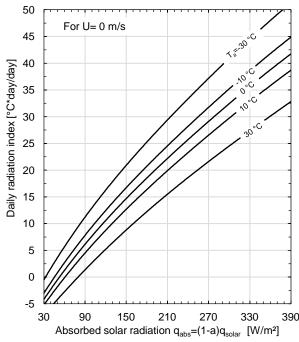
$$FI_s = FI_a - RI \qquad [6]$$

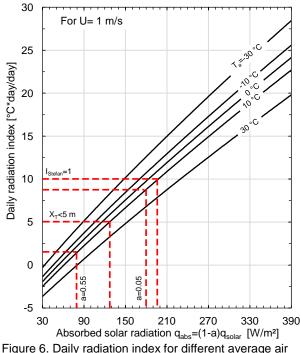where FI_s is the freezing index of the surface; and FI_a is the freezing index of the air.

$$TI_s = TI_a + RI \qquad [7]$$

where TI_s is the thawing index of the surface; and TI_a is the thawing index of the air.

Figure 5 to 8 present charts to calculate the daily radiation index (RI_{daily}) from the absorbed solar radiation for different average air temperature (T_a) and different wind speed. These charts can be used to find the radiation index of time step of any length (e.g., daily, weekly, and monthly). The total radiation index can be calculated by multiplying the daily radiation index by the total number of days of the time-step used.

Figure 5. Daily radiation index for different average air temperature for U=0 m/s

Figure 6. Daily radiation index for different average air temperature for U=1 m/s (dashed lines from example 5.1)
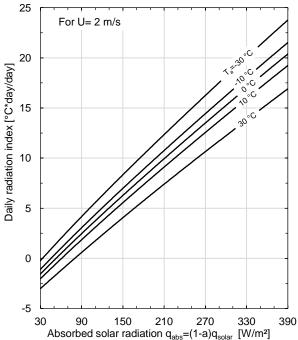
Figure 7. Daily radiation index for different average air temperature for U=2 m/s
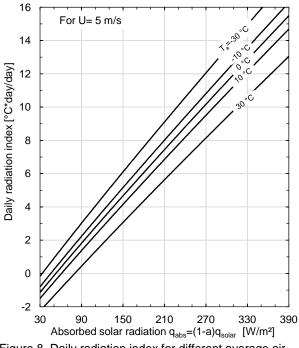

Figure 8. Daily radiation index for different average air temperature for U=5 m/s

4 STEFAN INDEX

The surface temperatures calculated using the previously described method can be used to assess the effectiveness of high albedo surfaces to prevent permafrost degradation for a specific site. They can be used directly in thermal modelling software to model thaw depth underneath the pavement surface. An index based on Stefan equation is also proposed here.

Stefan equation is presented in equation 8. It can be used to calculate the depth of thawing using the unfrozen thermal conductivity and the depth of freezing using the frozen thermal conductivity (Andersland and Ladanyi 2004, Aldrich and Paynter 1966).

$$X = \sqrt{\frac{2kT_s t}{L}} \qquad [8]$$

where X is the depth of thawing or freezing; k is the thermal conductivity of the soil; T_s, the surface temperature; t is the length of the time-step in days ;and L is the latent heat of the soil.

The Stefan index (I_{Stefan}) represents the ratio between the depth of thawing and the depth of freezing underneath the pavement surface and is presented in equation 9.

$$I_{Stefan} = \frac{X_F}{X_T} = \sqrt{\frac{k_f}{k_u}}\sqrt{\frac{FI_s}{TI_s}} \qquad [9]$$

where X_F is the freezing depth; X_T is the thawing depth; FI_s is the freezing index of the surface; and TI_s is the thawing index of the surface.

When the freezing depth is higher than the thawing depth, the Stefan index is higher than unity and the pavement acts as a heat sink helping to stabilize the embankment. Otherwise, the pavement represents a heat source which can induce permafrost degradation under the centerline of the road. The minimal value of albedo that warrants a Stefan index higher than one can easily be determined. Indeed, the freezing index of the surface is independent of the albedo, therefore the Stefan index is only affected by the albedo through the thawing index.

For a Stefan index equal to unity, equation 9 can be simplified:

$$\frac{TI_s}{FI_s} = \frac{k_f}{k_u} \qquad [10]$$

The proposed Stefan index only evaluates the effect of the albedo on the freezing and thawing depth underneath the pavement surface. Additional analysis are required to take into account various parameters involved in heat balance of embankments, such as snow accumulation, presence of insulation and water management along the embankment.

5 WORKING EXAMPLES

Two working examples are presented here. The first one is for Beaver Creek, Yukon for which all climatic data are available. The second one is for Iqaluit, Nunavut for which normal climatic data are available but the incoming solar radiation is unavailable and will be calculated.

The same typical values of thermal conductivities of highway embankment granular material are used in both examples (Côté and Konrad 2005). The unfrozen thermal conductivity used is 1.78 W/m°C. The frozen thermal

conductivity used is 1.88 W/m°C. The latent heat of the soil used is 29 MJ/m³.

Different parameters will be studied for Beaver Creek and Iqaluit. First, the minimal albedo to attain a Stefan index equal to unity will be calculated. Second, the case of a 5 meters high embankment will be studied. The minimal albedo required to limit the maximal thaw depth to 5 meters will thus be calculated. Finally, the Stefan index and surface temperature will be calculated for a typical new asphalt pavement with an albedo value of 0.05 and for a highly reflective pavement with an albedo value of 0.55.

5.1 Beaver Creek, Yukon

Table 1 presents the climactic data used for the Beaver Creek example. The normal climatic data were used for the air temperature (Environment Canada 2015). The incoming solar radiation and the wind speed were monitored as part of the validation process of the model presented in section 2 (Dumais 2014).

Table 1. Climatic data for Beaver Creek

FI_a	3322 °C·days
$t_{freezing}$	212 days
TI_a	1574 °C·days
$t_{thawing}$	153 days
$q_{inc\_thawing}$	180 W/m²
U	1 m/s

5.1.1 a_{min} for $I_{Stefan}=1$

Equation 10 can be used to calculate the thawing index of the surface yielding a Stefan index of 1 when an n-factor of 0.9 as suggested by Dumais (2014) is used to calculate the freezing index of the surface:

$$\frac{TI_S}{0.9 \times 3322} = \frac{1.88}{1.78} \qquad [11]$$

The radiation index can then be calculated from equation 7:

$$TI_S = TI_a + RI = 3158 \ °C \cdot days \qquad [12]$$

$$RI = 3158 - 1574 = 1584 \ °C \cdot days. \qquad [13]$$

The daily radiation index is:

$$\frac{RI}{t_{thawing}} = \frac{1584}{153} \approx 10 \ °C \cdot \frac{days}{days}. \qquad [14]$$

The average air temperature during the thawing season is:

$$\frac{TI_a}{t_{thawing}} = \frac{1574}{153} \approx 10 \ °C. \qquad [15]$$

The absorbed solar radiation can be found from the daily radiation index in figure 6 for the wind speed equal to

1 m/s and the curve of average air temperature equal to 10°C:

$$q_{abs} = 195 \frac{W}{m^2}. \qquad [16]$$

The minimal albedo required to have a Stefan index equal to unity is calculated using equation 2:

$$q_{abs} = (1-a) \times q_{inc} = 195 \frac{W}{m^2}, \qquad [17]$$

$$a = 1 - \frac{195}{180} < 0. \qquad [18]$$

A pavement with any albedo value will ensure that the thaw depth is smaller than the freezing depth within the embankment for the Beaver Creek climatic conditions.

5.1.2 a_{min} for $X_T<5$ m

Stefan equation (equation 8) can be used directly to find the thawing index of the surface that limits the thaw depth to 5 meters:

$$X = \sqrt{\frac{2k_u T_s t}{L}} = 5 \ m, \qquad [19]$$

$$TI_S \approx 2360 \ °C \cdot days. \qquad [20]$$

The radiation index is 790 °C·days and the daily radiation index is about 5 °C·days/days which gives a value of absorbed solar radiation of 127 W/m² and a minimal albedo value of about 0.3.

A pavement with an albedo of 0.3 or higher will limit the thaw depth at 5 meters for the Beaver Creek climatic conditions.

5.1.3 I_{Stefan} with a=0.05 and a=0.55

The Stefan index can be calculated for pavement with specific albedo values of 0.05 and 0.55. The absorbed solar radiation is calculated using equation 2:

for a=0.05
$$q_{abs} = (1-a)q_{inc} = (1-0.05) \times 180 = 171 \frac{W}{m^2}, \qquad [21]$$

and for a=0.55
$$q_{abs} = (1-a)q_{inc} = (1-0.55) \times 180 = 81 \frac{W}{m^2}. \qquad [22]$$

The daily radiation index is then found on figure 6 for the wind speed equal to 1 m/s and the curve of average air temperature equal to 10°C. The daily radiation index is multiplied by the number of days of the thawing season to find the total radiation index and the thawing index of the surface:

for a=0.05
$$TI_S = TI_a + RI$$
$$= 1574 + 7.5 \times 153 = 2722 \ °C \cdot days, \qquad [23]$$

for a=0.55
$$TI_S = TI_a + RI$$

$$= 1574 + 3 \times 153 = 2033 \,°C \cdot days. \qquad [24]$$

The average surface temperature of the pavement during the thawing season is:

for a=0.05
$$T_s = \frac{2722}{153} = 17.8 \,°C, \qquad [25]$$

for a=0.55
$$T_s = \frac{2033}{153} = 13.3 \,°C, \qquad [26]$$

The Stefan Index can then be calculated with equation 9:

for a=0.05
$$I_{Stefan} = \sqrt{\frac{k_f}{k_u}} \sqrt{\frac{FI_s}{TI_s}} = \sqrt{\frac{1.88}{1.78}} \sqrt{\frac{0.9 \times 3322}{2722}} = 1.08, \qquad [27]$$

for a=0.55
$$I_{Stefan} = \sqrt{\frac{k_f}{k_u}} \sqrt{\frac{FI_s}{TI_s}} = \sqrt{\frac{1.88}{1.78}} \sqrt{\frac{0.9 \times 3322}{2033}} = 1.25, \qquad [28]$$

As anticipated from the results of section 5.1.1 both pavement have a Stefan index higher than 1 and both pavement ensure that the thaw depth is smaller than the freezing depth.

5.2 Iqaluit, Nunavut

Table 2 presents the climactic data used for the Iqaluit example (Environment Canada 2015).

Table 2. Climatic data for Iqaluit

FI_a	4052 °C·days
$t_{freezing}$	243 days
TI_a	695 °C·days
$t_{thawing}$	122 days
Latitude	63°45' N
$n/N_{thawing}$	0.3
U	4 m/s

5.2.1 Incoming solar radiation

For Iqaluit, the incoming solar radiation for the thawing season is unavailable. It can be calculated using figure 3 and equation 5:

$$\begin{aligned} q_{solar} &= G_0(0.25 + 0.54 \cdot n/N) \\ &= 330(0.25 + 0.54 \times 0.3) = 136 \, W/m^2 \end{aligned} \qquad [12]$$

For the freezing season the incoming solar radiation can be calculated using figure 4 and equation 5:

$$\begin{aligned} q_{solar} &= G_0(0.25 + 0.54 \cdot n/N) \\ &= 80(0.25 + 0.54 \times 0.3) = 33 \, W/m^2 \end{aligned} \qquad [12]$$

The n-factor approach will be preferable for Iqaluit as the solar radiation is close to the threshold value of 30 W/m². A conservative n-factor value of 0.9 will be used (Dumais, 2014).

5.2.2 Summary of Iqaluit results

Table 3 presents all the different parameters calculated as in example 5.1 by using interpolated radiation index values between figure 7 and 8 because of the wind speed which is 4 m/s.

Table 3. Results for Iqaluit

a_{min} for $I_{Stefan}=1$	0.00
a_{min} for $X_T<5$ m	0.00
I_{Stefan} for a=0.05	1.83
T_s for a=0.05	9.4 °C
I_{Stefan} for a=0.55	2.31
T_s for a=0.55	5.9 °C

The Stefan indices are relatively high due to the large freezing index of the air in Iqaluit.

5.3 Discussion on working examples

The results from both working examples outline how the climatic conditions affects the surface temperatures of the pavement and the efficiency of high albedo surfaces. For Beaver Creek, the thawing season is long and the incoming solar radiation is significant. Whereas for Iqaluit, the combined effect of the high wind speed and of a very low cloud factor that reduces the incoming solar radiation reduce greatly the surface temperature of the pavement. The albedo of the pavement is thus a bigger concern in Beaver Creek than in Iqaluit. High albedo surfaces are generally more effective for long and cool thawing season when the solar radiation is high (Dumais 2014).

6 CONCLUSION

In conclusion, a method for the calculation of surface temperature of pavements in permafrost regions was proposed. This method is based on a previously validated model and uses the radiation index approach. A method to calculate the incoming solar radiation was discussed. Convenient and reliable design charts were proposed in order to efficiently calculate the radiation index of a surface. An index based on Stefan equation was proposed in order to quickly asses the effectiveness of high albedo surfaces for a specific site by evaluating the ratio between the penetration of thawing and freezing under the pavement surface. Two working examples were presented to show how to use the proposed method. These examples outlined how climatic conditions impact the effectiveness of high albedo surfaces.

REFERENCES

Akbari, H., Levinson, R., and Stern, S., 2008. Procedure for measuring the solar reflectance of flat or curved roofing assemblies. *Solar Energy Materials & Solar Cells*, 82: 648–655.

Aldrich, H. P., Jr., and H. M. Paynter. 1966. Depth of Frost Penetration in Non-uniform Soil. *U.S. Army Cold Regions Research and Engineering Laboratory Special Report 104.*

Andersland, O. B., and Ladanyi, B. 2004. *Frozen ground engineering,* 2nd ed., ASCE and John Wiley & Sons Inc., Hoboken, NJ, USA.

ASTM, 2006. ASTM E1918-06: Standard Test Method for Measuring Solar Reflectance of Horizontal and Low-Sloped Surfaces in the Field. American Society for Testing and Materials, West Conshohocken, PA, USA.

Berg, R. L., and W. F. Quinn. 1977. Use of a light-colored surface to reduce seasonal thaw penetration beneath embankments on permafrost. *Proc. 2nd Int. Symp. on Cold Regions Engineering*, University of Alaska, 1: 86–99.

Bjella, K. 2013. An Investigation into a White Painted Airfield on Permafrost: Thule Air Base, Greenland. *ISCORD 2013,* ASCE, 1: 565-575.

Côté, J., and Konrad, J.-M. 2005. Thermal conductivity of base-course materials. *Can. Geotech. J.*, 42(1): 61–78.

Dumais, S. 2014. Évaluation des revêtements routiers à albédo élevé en contexte nordique. Master Thesis, Université Laval, Québec, Québec, Canada.

Dysli, M. 1991. *Le gel et son action sur les sols et les fondations.* Presses Polytechniques et Universitaires Romandes, Lausanne, Switzerland.

Environnement Canada. 2015. *Canadian Climate Normals 1981-2010 Station Data.* climate.weather.gc.ca. Government of Canada.

Kilokotsa, D. D., M. Santamouris, and H. Akbari. 2013. Advances in the Development of Cool Materials for the Built Environment. Bentham eBooks. 5: 104-119.

Levinson, R., Akbari, H., Berdahl, P., 2010a. Measuring solar reflectance—Part I: Defining a metric that accurately predicts solar heat gain. *Solar Energy*, 84: 1717-1744.

Levinson, R., Akbari, H., Berdahl, P., 2010b. Measuring solar reflectance—Part II: Review of practical methods. *Solar Energy,* 84 :1745-1759.

Prescott, J.A. 1940. Evaporation from a water surface in relation to solar radiation. *Trans. R. Soc. South Australia*, 64:114-118.

Siegel, R., Howell, J., 2002. *Thermal Radiation Heat Transfer*, 4th ed., Taylor & Francis.